AEM
Journals.ASM.org

Adaptation Genomics of a Small-Colony Variant in a *Pseudomonas chlororaphis* 30-84 Biofilm

Dongping Wang,[a] Robert J. Dorosky,[b] Cliff S. Han,[a] Chien-chi Lo,[a] Armand E. K. Dichosa,[a] Patrick S. Chain,[a] Jun Myoung Yu,[b] Leland S. Pierson III,[b] Elizabeth A. Pierson[b,c]

Bioscience Division, Los Alamos National Laboratory, Los Alamos, New Mexico, USA[a]; Departments of Plant Pathology and Microbiology[b] and Horticultural Sciences,[c] Texas A&M University, College Station, Texas, USA

The rhizosphere-colonizing bacterium *Pseudomonas chlororaphis* 30-84 is an effective biological control agent against take-all disease of wheat. In this study, we characterize a small-colony variant (SCV) isolated from a *P. chlororaphis* 30-84 biofilm. The SCV exhibited pleiotropic phenotypes, including small cell size, slow growth and motility, low levels of phenazine production, and increased biofilm formation and resistance to antimicrobials. To better understand the genetic alterations underlying these phenotypes, RNA and whole-genome sequencing analyses were conducted comparing an SCV to the wild-type strain. Of the genome's 5,971 genes, transcriptomic profiling indicated that 1,098 (18.4%) have undergone substantial reprograming of gene expression in the SCV. Whole-genome sequence analysis revealed multiple alterations in the SCV, including mutations in *yfiR* (cyclic-di-GMP production), *fusA* (elongation factor), and *cyoE* (heme synthesis) and a 70-kb deletion. Genetic analysis revealed that the *yfiR* locus plays a major role in controlling SCV phenotypes, including colony size, growth, motility, and biofilm formation. Moreover, a point mutation in the *fusA* gene contributed to kanamycin resistance. Interestingly, the SCV can partially switch back to wild-type morphologies under specific conditions. Our data also support the idea that phenotypic switching in *P. chlororaphis* is not due to simple genetic reversions but may involve multiple secondary mutations. The emergence of these highly adherent and antibiotic-resistant SCVs within the biofilm might play key roles in *P. chlororaphis* natural persistence.

Pseudomonas chlororaphis 30-84 is a rhizosphere bacterium that is effective against take-all disease of wheat, which is caused by the soilborne fungal pathogen *Gaeumannomyces graminis* var. *tritici*. *P. chlororaphis* 30-84 produces several secondary metabolites, including phenazines, that contribute to pathogen inhibition and persistence in the rhizosphere (1). Previous studies revealed additional critical roles of phenazines. For instance, phenazines are involved in bacterial biofilm formation (2). Phenazines also serve as signals and have been shown to regulate the expression of more than 50 genes in the opportunistic pathogen *Pseudomonas aeruginosa* and 200 genes in *P. chlororaphis* 30-84, respectively (3; D. Wang and E. A. Pierson, unpublished data). Additionally, phenazines have been shown to induce plant defense pathways and play a role in electron shuttling and iron chelation (4–6).

Many bacteria establish long-term populations on their hosts or within specific environments. One strategy for bacterial persistence is the formation of biofilms, bacterial aggregates embedded in a self-produced matrix (7). Compared to free-living cells, the cells living in the biofilm microenvironment may be exposed to smaller amounts of free iron, oxygen, and nutrients (7, 8). To cope with these limiting factors, genes involved in stress response, iron uptake, low oxygen growth, and antibiotic resistance are highly induced under biofilm conditions (7, 8).

Many *Pseudomonas* species undergo phenotypic diversification while adapting to the biofilm environment (9, 10). Small-colony variants (SCVs) are slow-growing (low metabolic activity) isolates commonly characterized by several phenotypes, including chromatin aggregation, high adherence, and enhanced antimicrobial resistance (11). SCVs have been isolated in a wide array of bacterial species, including *Pseudomonas aeruginosa* (11–13) and *Pseudomonas fluorescens* (14). The occurrence of SCVs generally correlates with prolonged persistence and increased antibiotic resistance. A recent analysis of the spatial distribution of *P. fluorescens* SCVs in mixed-culture biofilms with the wild type (WT) reveals that SCVs demonstrate a significant growth advantage over the WT in the biofilm environment (14). The variant strains displaced the WT across the entire biofilm, and this occurred within 24 h. Interestingly, this competitive growth advantage was not observed in homogeneous broth culture. These results further reinforce the hypothesis that SCVs are particularly adapted to the biofilm environment. The SCVs of some strains can phenotypically switch back to the wild-type morphology under certain environmental conditions (11). However, the molecular mechanisms underlying this phenomenon are not well studied, especially at the genomic level.

Whole-genome sequencing and microarray studies also suggest that SCVs adapt genetically and transcriptionally to specific environmental stresses, e.g., antibiotic treatment or nutrient limitation. In *P. aeruginosa* PAO1, SCVs contained mutations in the elongation factor *tufA* (11) and the cyclic-di-GMP (c-di-GMP) regulator *yfiR* (15). Importantly, the deletion of *yfiR* in strain

Received 8 August 2014 **Accepted** 13 November 2014

Accepted manuscript posted online 21 November 2014

Citation Wang D, Dorosky RJ, Han CS, Lo C, Dichosa AEK, Chain PS, Yu JM, Pierson LS, III, Pierson EA. 2015. Adaptation genomics of a small-colony variant in a *Pseudomonas chlororaphis* 30-84 biofilm. Appl Environ Microbiol 81:890–899. doi:10.1128/AEM.02617-14.

Editor: R. M. Kelly

Address correspondence to Dongping Wang, dwang22@lanl.gov, or Elizabeth A. Pierson, eapierson@tamu.edu.

Supplemental material for this article may be found at http://dx.doi.org/10.1128/AEM.02617-14.

Copyright © 2015, American Society for Microbiology. All Rights Reserved.

doi:10.1128/AEM.02617-14

Downloaded from http://aem.asm.org/ on September 11, 2018 by guest

PAO1 resulted in the formation of SCVs and elevated c-di-GMP levels, which indicated a key role of cyclic-di-GMP in phenotypic variation (15). YfiR is one of two negative regulators of YfiN, a diguanylate cyclase originally named TpbB (16). TpbB/YfiN also is controlled by the phosphatase TpbA, and activation of TpbB/YfiN by inactivation of TpbA causes SCV formation (16). These data suggest that YfiR-TbpA-TbpB/YifN pathways can be linked to the SCV phenotype in *P. aeruginosa*. In addition to genetic changes, SCVs also undergo substantial transcriptional reprograming. Microarray analyses have been conducted to identify genes responsible for the pleiotropic phenotypes observed in SCVs. In *P. aeruginosa* PAO1, 642 genes, representing ~12% of the entire genome, were differentially expressed in an SCV compared with the WT (11). These include genes involved in antibiotic resistance and quorum sensing, which often contribute to the multidrug resistance phenotype. Another study comparing the transcriptome of *P. aeruginosa* 20265 with its SCV derivative indicated changes in the expression levels of genes involved in motility, attachment, virulence, and iron uptake (17). Genome sequencing and transcriptome approaches to understanding adaptation should provide important complements to phenotypic studies of bacterial SCVs (18).

In this study, we examined the transcriptional and genomic alterations associated with the SCV phenotype in the beneficial root-colonizer *P. chlororaphis* 30-84. Genome analysis of a phenotypic revertant strain also was performed to identify genes potentially involved in phenotypic switching. This work comprises a genome-wide evolutionary analysis of a phenotypic switching event in *P. chlororaphis*. Genes identified by genomic or transcriptomic approaches will provide novel insights to better understand genetic adaptations during biofilm formation.

MATERIALS AND METHODS

Bacterial strains and growth conditions. The *P. chlororaphis* SCVs used for this study were isolated from biofilm cultures of WT *P. chlororaphis* 30-84. Briefly, bacteria were grown overnight in LB medium and then inoculated at a ratio of 1:150 into 15 ml 15- by 100-mm glass tubes containing 1.5 ml LB. Tubes were incubated without shaking for 6 days to induce static biofilm formation. Phenotypically identical SCVs accounting for ~50% of the total population were consistently isolated from independent biofilm cultures. More than a dozen SCVs from independent biofilm cultures were isolated, and one of the SCVs was selected for this study. Phenotypic revertants were generated by incubating the SCV strain on swimming motility plates (LB medium; 2.5 g agar per liter distilled water). After 3 days of incubation, cells having the wild-type morphology (e.g., phenotypic revertants) were isolated from the edge of the swimming circle, and one was selected for further analysis. Primers used for PCR are listed in Table S1 in the supplemental material. LB medium or AB minimal medium supplemented with 2% Casamino Acids (AB plus 2% CAA) (Difco, Becton Dickinson and Company, Franklin Lakes, NJ) was used for culturing *P. chlororaphis* as described previously (19).

PCR and sequence analysis. PCR was carried out using *Taq* DNA polymerase (Invitrogen Life Technologies) at 95°C for 5 min, followed by 30 cycles of 95°C for 30 s, 60°C for 30 s, and 72°C for 90 s, and then a final elongation step of 70°C for 10 min. Nucleotide and amino acid homology searches were conducted using the blast programs at the National Center for Biotechnology Information (NCBI) (http://www.ncbi.nlm.nih.gov/BLAST). The *P. chlororaphis* 30-84 phenazine biosynthetic operon contains seven conserved biosynthetic genes *phzXYFABCD* (according to the original nomenclature [19, 20]), which correspond to *phzABCDEFG* (according to the *P. fluorescens* nomenclature). Here, we use the *P. chlororaphis* nomenclature to conform to the original literature.

Cloning *yfiR*, *cyoE*, *bifA*, and *fusA* genes from *P. chlororaphis*. For *yfiR*, *fusA*, and *cyoE* complementation, flanking sequences of the open reading frames (ORFs) in the *P. chlororaphis* WT were used to design primers to amplify fragments of the genes and their promoter sequences. Primer pairs yfiR-F–yfiR-R, fusA-F–fusA-R, and cyoE-F–cyoE-R were used to amplify DNA fragments from the *P. chlororaphis* WT strain, containing upstream and downstream sequences of *yfiR*, *fusA*, and *cyoE* genes, respectively (see Table S1 in the supplemental material). The PCR fragments were digested by restriction enzymes and cloned into the vector pProbeGT′ (pGT2) (19). The final plasmids were designated pYfiR, pFusA, and pCyoE, and their genotypes were confirmed by sequencing. All plasmids were introduced into the *P. chlororaphis* SCV by conjugation. Transformants were selected on LB plates supplemented with gentamicin. The *bifA* gene (with its promoter) was cloned from the phenotypic revertant using primers bifA-F and bifA-R (see Table S1). The resulting plasmid was introduced into the *P. chlororaphis* SCV by conjugation.

TEM. Transmission electron microscopy (TEM) was performed at the Microscopy and Imaging Center at Texas A&M University. Bacteria were grown in LB medium for 18 h. Cells from the media were applied directly to the TEM grid for 3 min. The grid was stained with a 2% aqueous solution of phosphotungstic acid for 1 min. Samples were examined using a Japan Electron Optics Laboratory (JEOL) 1200 transmission electron microscope at an acceleration voltage of 100 kV. The sizes of 10 fully developed *P. chlororaphis* 30-84 and SCV cells were measured and compared. All of the SCVs demonstrated dark areas in the centers of the cells.

Quantification of phenazine production. Bacterial strains were grown with aeration at 28°C in PPMD, LB, and AB minimal medium supplemented with 2% CAA for 24 h. Phenazines were extracted and quantified by UV-visible light spectroscopy as described previously (19). Briefly, triplicate 10-ml cultures grown overnight at 28°C with shaking in different media were centrifuged, and the supernatants were acidified to approximately pH 2 with concentrated HCl. Phenazines were extracted with an equal volume of benzene for 6 h. Following the evaporation of the benzene under air, phenazines were resuspended in 0.5 ml 0.1 M NaOH, and serial dilutions were quantified via measuring absorbance at 367 nm. The absorbance for each sample was normalized to the total absorbance of the 10-ml culture.

Pathogen inhibition assays. To measure the ability of the WT and SCV to inhibit the pathogen *G. graminis* var. *graminis*, overnight cultures of WT and SCV were spotted onto triplicate LB plates plus 0.5% potato dextrose agar. After 2 days of growth at 28°C, a 5-mm plug of *G. graminis* var. *graminis* was placed in the center of the plates. After 4 days, zones of inhibition, the distance between the edge of the bacterial colony and the fungal mycelium, were measured (19). The assays were repeated three times, and one representative experiment is presented. *P. chlororaphis* 30-84ZN, used as a negative control, carries a mutation in the *phzB* gene and is deficient in phenazine production.

Biofilm formation assay. Biofilm formation was determined as described previously, with slight modifications (2). Briefly, bacterial strains were grown overnight in LB at 28°C with agitation and diluted (1:100) in LB broth. Aliquots of 3 ml of the diluted culture were added to 15-ml polypropylene tubes, and the tubes were incubated at 28°C without shaking. After 48 h, the planktonic bacteria were carefully removed by pipetting, and the tubes were washed with water to remove bacteria that were not firmly attached to the polypropylene surface. To visualize biofilm formation, 3.5 ml of 1% (wt/vol) crystal violet (CV) was added to each tube, and the tubes were incubated at room temperature for 5 min before rinsing in tap water. To quantify biofilm formation, CV was dissolved into 4 ml/μl of acetone-ethanol (20:80), and the CV concentration was determined by measuring the OD_{540} of a 500-μl sample diluted in 1 ml of water.

Bacterial swimming motility assays. Bacterial cell suspensions were grown overnight in LB medium. A 4-μl volume of the bacterial suspension was plated onto the center of motility agar plates as previously de-

Downloaded from http://aem.asm.org/ on September 11, 2018 by guest

scribed (21). Diameters were determined following incubation at 28°C for up to 32 h. The experiments were repeated at least three times.

Antimicrobial killing assays. Bacterial strains were grown separately overnight in LB broth without antibiotics, collected by centrifugation at 5,000 × *g* for 10 min, and washed with 1× phosphate-buffered saline (PBS) three times. The pellets were resuspended in 200 μl of PBS, and 20-fold serial dilutions of bacterial suspensions were made in 96-well plates. Five-μl aliquots of the suspensions then were spotted separately on LB plates containing kanamycin (100 μg/ml), piperacillin (50 μg/ml), and hydrogen peroxide (3%) and incubated at room temperature for 3 days. The survival percentage was calculated by dividing antimicrobial-treated versus untreated colony-forming numbers. The dilution of each strain was carried out in triplicate. The experiment was repeated at least three times.

RNA preparation for RNA-seq and quantitative PCR (qPCR) analyses. Two (SCV) or three (WT) biological replicates were started from single colonies located on separate plates containing AB plus 2% CAA and then transferred to 1.5 ml AB plus 2% CAA broth. All cultures were grown at 28°C in shaking tubes to an approximate OD_{600} of 1.8. RNA extraction was performed as described previously (19). rRNA was depleted from ~5 μg of total RNA using the RiboZero rRNA depletion kit (for Gram-negative bacteria; Epicentre Biotechnologies, Madison, WI). RNA quantification was achieved using a GE NanoVue Plus spectrophotometer (GE Healthcare Bio-Sciences Corp., Piscataway, NJ), and RNA quality was monitored with an Agilent 2100 Bioanalyzer (Agilent Technologies, Santa Clara, CA). Separate libraries of the WT and SCV were created prior to RNA-sequencing (RNA-seq) analysis.

RNA-seq analysis. RNA-seq analysis was performed at Otogenetics, Atlanta, GA. Briefly, cDNA was generated from the rRNA-depleted RNA using the NEBNext mRNA sample prep kit (New England BioLabs, Ipswich, MA, USA). The resulting cDNA was profiled using an Agilent Bioanalyzer, fragmented using Covaris (Covaris, Inc., Woburn, MA, USA), and subjected to Illumina library preparation using NEBNext reagents (New England BioLabs, Ipswich, MA, USA). The quality and quantity and the size distribution of the Illumina libraries were determined using an Agilent Bioanalyzer 2100. The libraries then were submitted for Illumina HiSeq2000 sequencing according to the standard operation. Paired-end 90- or 100-nucleotide (nt) reads were generated and checked for data quality using FASTQC (Babraham Institute, Cambridge, United Kingdom).

Based on gene annotation information, reads were mapped to the genome, resulting in a compressed binary version of the sequence alignment map (BAM files). To determine the transcriptional abundance for each gene, the number of reads that mapped within each annotated coding sequence (CDS) was determined. The number of reads per kb of transcript per million mapped reads (RPKM) was used to normalize the raw data (21), and mean RPKM values were determined for both the wild-type and SCV samples. A ratio of the mean RPKM values (SCV/WT) was computed for each gene, and comparisons were performed using EdgeR (22). Genes were identified as being differentially expressed based on the RPKM ratios (SCV/WT) when the *P* value was less than 0.05 and the expression ratio was ≥2.0 or ≤0.5 (see Table S2 in the supplemental material).

qPCR methods and analysis. qPCR was performed at the Gene Expression Service Center at Texas A&M University using a previously described method (19). SYBR green reactions were performed using the ABI 7900 HT Fast system (Applied Biosystems, Foster City, CA) in 384-well optical reaction plates. Aliquots (1 μl) of cDNA (2 ng/reaction mixture) or water (no-template control) were used as the template for qPCRs with Fast SYBR green PCR master mix (Applied Biosystems) and primers (500 nM final concentration). Primer pairs katART1-katAYRT2, katBRT1-katBRT2, pvdART1-pvdART2, fppART1-fppART2, phzBRT1-phzBRT2, fusART1-fusART2, cyoERT1-cyoERT2, fliCRT1-fliCRT2, phzRRT1-phzRART2, rpoDRT1-rpoDRT2, and hfqRT1-hfqRT2 were used to detect the expression of *katA*, *katB*, *pvdA*, *fppA*, *phzB*, *fusA*, *cyoE*, *fliC*, *phzR*, *rpoD*, and *hfq* genes, respectively (see Table S1 in the supplemental material). qPCR amplifications were carried out at 50°C for 2 min, 95°C for 10 min, 40 cycles of 95°C for 15 s and 60°C for 1 min, and a final dissociation curve analysis step from 65°C to 95°C. Technical replicate experiments were performed for each biological triplicate sample. Amplification specificity for each reaction was confirmed by dissociation curve analysis. Determined threshold cycle (C_T) values then were used for further $\Delta\Delta C_T$ analysis. The *hfq* and *rpoD* genes were used as the reference genes to normalize samples. The fold differences in the expression of target genes between the WT and SCV were comparable using either *hfq* or *rpoD* as the reference gene. A relative quantification (RQ) value was calculated for each gene, with the control group as a reference (19, 21).

Genome sequencing and identification of genetic variations. Genome sequencing was performed using a MiSeq sequencer with 250-bp read chemistry (Illumina). A modified TruSeq DNA Sample Prep v2 and MiSeq sequencing protocol was used during the sequencing process (23). Briefly, genomic DNA from the WT, SCV, and the phenotypic revertant was isolated from overnight cultures using the DNeasy Miniprep kit (Qiagen, Hilden, Germany). The genomic library was constructed using 1 μg of genomic DNA fragmented by a Covaris E210 instrument. The samples then were run on a gel and size selected for a range of 400 to 500 bp to accommodate the longer read length capability of the MiSeq sequencer. The size-selected library underwent 10 cycles of PCR. The libraries were quantified using the Qubit double-stranded DNA high-sensitivity assay (Invitrogen, Carlsbad, CA, USA). The sequencing program was set up to generate 2-by-250 base-paired reads.

MiSeq sequencing generated a total of 6,954,294 reads. The reads were mapped to the reference genome of *P. chlororaphis* 30-84 (NCBI accession number NZ_CM001559). The reads were trimmed using the Perl script illumina_fastq_QC.pl (https://github.com/chienchi/IFQC) with a quality threshold of 5 to remove sequences of low read quality or sequences with adapters. The program also filtered reads with more than two continuous ambiguous bases and low-complexity reads (mono/dinucleotide repeats). The Burrows-Wheeler Aligner software (default parameters; version 0.6.2-r126-tpx) (24) was used to map Illumina reads to the *P. chlororaphis* 30-84 genome. This software includes a gapped alignment algorithm, which improves the detection of indel read pairs (90.67% of the original reads). Reads were mapped to unique locations, resulting in a median read depth (genome coverage) of 46. Single-nucleotide polymorphisms (SNPs) and indels were detected with SAMtools software (version 0.1.19) using its built-in function "mpileup" and the "bcftools view" and "vcfutils.pl varFilter" commands in a pipeline to call the SNPs (24). Custom scripts developed by the Los Alamos National Laboratory were used to filter the variants based on a minimum overall quality of 20 reads and variant location in the repeats. The resulting SNPs/indels and zero-covered regions of the reference genome were compared with GenBank annotation to report affected genes.

GEO accession number. The complete data set from this study has been deposited in the NCBI Gene Expression Omnibus (GEO) under accession no. GSE51293.

RESULTS

Phenotypic characterization of a *P. chlororaphis* SCV. (i) Cell morphology and growth. The colony morphologies of the WT and SCV on LB agar plates are shown in Fig. 1A. Isolated colonies formed by WT *P. chlororaphis* after 3 days of incubation at 28°C are round (~4.0 ± 1.1 mm in size), with smooth, regular margins. In contrast, SCV colonies appear rugged and small (~0.6 ± 0.5 mm in diameter). Morphological differences were reflected at the single-cell level (Fig. 1B). Typically present in the center of SCV cells was a dark area not found in WT cells grown under these environmental conditions, possibly due to the condensation of the nucleoid. Reduced metabolic activity and slower growth are characteristic of SCVs of many bacterial species (18). Consistent

Downloaded from http://aem.asm.org/ on September 11, 2018 by guest

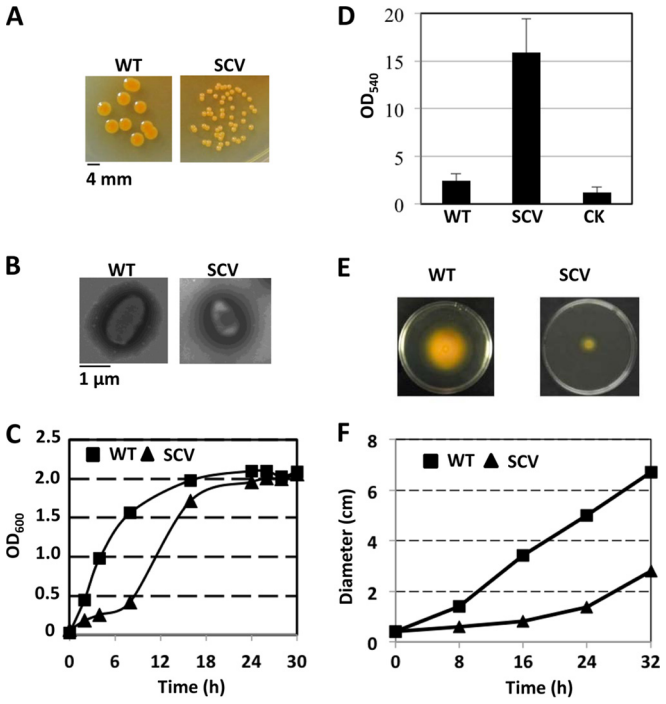

FIG 1 Phenotypes of SCV. (A) Comparison of colony sizes of *P. chlororaphis* WT and SCV. Bacteria were grown on an LB plate for 3 days. (B) Transmission electron microscopy analysis of cell morphology for *P. chlororaphis* WT and SCV. Bacteria were grown with shaking at 200 rpm and 28°C in LB medium to an OD_{600} of 1.8. Cells were negatively stained with 1% phosphotungstic acid (pH 7.0), and micrographs were taken at an accelerating voltage of 100 kV. One photo of a representative cell for each strain was selected. (C) Growth curves of *P. chlororaphis* WT and SCV in LB broth at 28°C. Original inocula from stationary cultures were inoculated at a volume-to-volume ratio of 1:1,000. (D) Biofilm formation by *P. chlororaphis* WT and SCV. Bacterial strains were grown overnight in LB broth at 28°C and diluted (1:100) in fresh LB media, and aliquots of 3-ml bacterial cultures were incubated at 28°C, without shaking, in 15-ml falcon tubes. After 48 h, liquid cultures were decanted, and cells in biofilms adhering to the side of the tubes were stained with 1% crystal violet (CV). The amount of CV staining was quantified at OD_{540}, and bars indicate standard errors (SE). Biofilm production was normalized to an OD_{600} of 1 for both the WT and SCV. CK, no bacteria. (E) Motility comparison of *P. chlororaphis* WT and SCV. Bacterial strains were spotted at the center of the motility plate (0.25% agar) and incubated at 28°C. Pictures were taken at 24 h postinoculation. (F) Comparison of swimming distances. The diameters of the swimming circle were measured at 8, 16, 24, and 32 h postinoculation. Standard error bars were smaller than the symbols. Data points represent means ± SE from nine biological replicates in three independent experiments.

with this, the SCVs of *P. chlororaphis* 30-84 grown in liquid LB entered the exponential phase later than the WT; thus, they displayed a longer lag phase (Fig. 1C).

(ii) *P. chlororaphis* SCV produces smaller amounts of phenazines than the wild type. Phenazine production was quantified by spectrophotometric assays for bacteria grown in AB minimal medium plus 2% Casamino Acids (19). Phenazine production by SCV (2.1 ± 0.4 at OD_{367}) was significantly reduced compared to that of the WT (3.5 ± 0.3 at OD_{367}). The production of phenazines is largely responsible for the ability of *P. chlororaphis* 30-84 to inhibit the growth of fungal pathogens (20). The ability to inhibit the growth of the plant pathogen *G. graminis* was determined using an *in vitro* plate inhibition assay. The WT strain produced a fungal inhibition zone of approximately 7.5 ± 0.9 mm at 4 days postinoculation, whereas the phenazine-defective mutant *P. chlororaphis* 30-84ZN resulted in significantly low inhibition (inhibition zone, 1.0 ± 0.6 mm). Consistent with low levels of phenazine production, the SCV also was diminished in its ability to inhibit the fungal growth at 4 days postinoculation, producing a mean inhibition zone of 3.2 ± 0.7 mm.

(iii) *P. chlororaphis* SCV is sessile and highly adhesive. Previous studies demonstrated that SCVs typically are reduced in motility but increased in surface attachment (11, 12). To determine whether *P. chlororaphis* SCVs are altered in attachment, the ability of the wild type and SCV to form biofilms on a water-air interface was evaluated using a standardized crystal violet method (2). Analysis revealed that biofilms (attached bacterial cells) formed by the SCV were 7-fold greater than those of the WT strain (Fig. 1D). These results confirm that *P. chlororaphis* SCV cells are highly adhesive to solid surfaces.

Bacterial motility by the wild type and SCV was measured by inoculating bacterial cells on a motility plate (0.25% agar) and measuring the diameter of the circle covered by bacterial cells for up to 32 h, as described previously (21). The SCV was almost completely defective in motility compared with the WT (Fig. 1E). The diameters of circles delimiting WT and SCV populations were 6.7 ± 0.2 and 2.8 ± 0.1 cm, respectively (Fig. 1F). These results demonstrate that the SCV of *P. chlororaphis* 30-84 also is impaired in motility.

(iv) *P. chlororaphis* SCV has enhanced antimicrobial resistance compared to the wild type. One of the most remarkable features of SCVs is enhanced antimicrobial resistance (18). To determine whether the *P. chlororaphis* SCV is more resistant to antimicrobials, WT and SCV were tested for their sensitivity to kanamycin, piperacillin, and hydrogen peroxide, and the survival rates of each strain were determined. On LB plates, the growth of wild-type *P. chlororaphis* was inhibited at a kanamycin concentration of 25 μg/ml or above (Fig. 2A). In contrast, the SCV grew even at 100 μg/ml. The SCV also was more resistant to piperacillin and hydrogen peroxide (Fig. 2B). The survival rates of the WT were 0%, 12%, and 32% when grown with kanamycin, piperacillin, and hydrogen peroxide, respectively, whereas those of SCV were increased to 93%, 74%, and 75%, respectively. These results indicate that the *P. chlororaphis* SCV is more resistant to a range of antimicrobials.

Global gene expression profiles in the SCV. To further define the causes for the phenotypic differences observed between the wild type and SCV, an RNA-seq approach was utilized to identify genes differentially expressed. We compared the SCV to the WT grown in AB minimal medium with 2% CAA at 18 h in late exponential growth. RNA-seq data (short reads) were aligned to the genome, and gene expression values were quantified as reads per kilobase of coding sequence (CDS) length per million reads (RPKM), as described previously (21). In order to identify genes differentially expressed in SCV, mean RPKM values for the SCV were compared with those for the WT using EdgeR (22). A total of 1,098 genes exhibited altered expression profiles in the SCV relative to the WT strain. Among them, 727 genes were upregulated and 371 genes were downregulated, indicating extensive transcriptional reprogramming in SCV cells (see Table S2 in the supplemental material).

Transcription of genes involved in specific metabolic functions was reduced in the SCV compared to that of the WT. It has been proposed that condensed chromatin contributes to the low

Downloaded from http://aem.asm.org/ on September 11, 2018 by guest

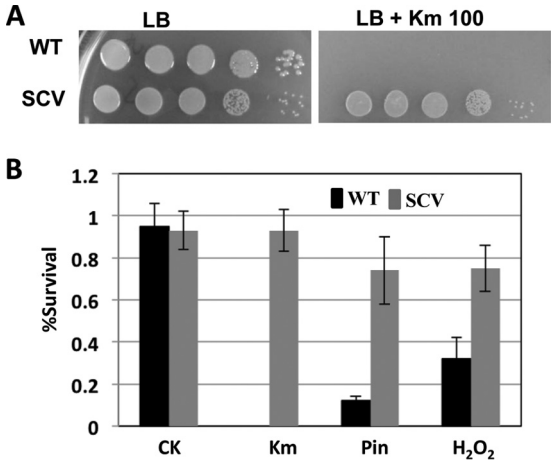

FIG 2 Antimicrobial killing assays. (A) Kanamycin sensitivity test on LB plates. Bacteria were grown with shaking at 28°C in LB medium to an OD_{600} of 0.5 and then diluted 1/20 a total of 5 times. Aliquots (10 μl) of different bacterial cells were spotted on LB plates with/without 100 μg/ml kanamycin. Pictures were taken at 3 days postinoculation. (B) Survival rates in response to different antimicrobials. Serially diluted WT and SCV were plated on LB agar plates containing 100 μg/ml kanamycin (Km), 50 μg/ml piperacillin (Pin), and 3% hydrogen peroxide (H_2O_2). Surviving bacterial cells were counted after 3 days of incubation. Data points represent the means from three biological replicates ± standard errors.

metabolic activity observed among the SCVs of some bacteria (25). One possibility is that condensed chromatin results in the decreased expression of metabolic genes. Consistent with this hypothesis, the expression of genes involved in primary metabolism was lower in the SCV than in the WT strain (see Table S3 in the supplemental material). These included genes that may be involved in housekeeping functions, such as protein translation (18 genes), transcription (2 genes), energy production (16 genes), and cell division (2 genes). These results further support the notion that *P. chlororaphis* 30-84 SCVs are less metabolically active than the WT.

SCV showed differential expression of genes involved in biofilm formation. Consistent with the measured reduction in phenazine production, the phenazine biosynthetic genes were downregulated 2- to 4-fold in the SCV (see Table S4 in the supplemental material). In *P. chlororaphis* 30-84, phenazine expression is regulated by a complex regulatory network, including quorum sensing (*phzI-phzR* and *csaI-csaR*), two-component regulatory systems (*rpeA-rpeB* and *gacS-gacA*), the phenazine-inducing protein (*pip*), the sigma factor *rpoS*, and the noncoding RNA *rsmZ* (19). Interestingly, the expression of these genes was not differentially changed in the SCV relative to the WT (data not shown). These data suggest that phenazine production is regulated by an as-yet unknown mechanism in the SCV. Since phenazines positively control biofilm formation, the reduction of phenazine synthesis in the SCV should decrease the level of biofilm formation. Interestingly, the SCV produced more surface-attached biofilm than the WT. These results suggest that surface-attached biofilm in the SCV is controlled by genes and traits in addition to phenazines. Indeed, the expression of an 11 gene cluster annotated as a type IV pili biosynthesis cluster was 2- to 15-fold higher in the SCV than in the WT (see Table S4 in the supplemental material). It has been shown that type IV pili function in *P. aeruginosa* twitching motility and attachment (17). It is possible that the overexpression of these genes confers greater adherence ability in SCV. The motility of *P. chlororaphis* 30-84 requires flagellar genes, and mutation in the *fliM* gene completely abolished motility (21). Transcript abundances of seven flagellar genes were lower in the SCV than in the WT (see Table S4). These genes are annotated as encoding the flagellar hook-associated protein (FlgK and FlgL), the flagellar motor switch protein (FliG), the flagellar assembly protein (FliH), the flagellum-specific ATP synthase (FliI), the flagellar export protein (FliJ), and flagellin (FliC). This is in agreement with the reduced swimming motility of SCV. Moreover, it was proposed that the reduction of flagella helps to stabilize the three-dimensional structure of the mature biofilm (5). The enhanced ability of SCV to form biofilms may be a consequence of the differential expression of genes involved in the production of pili and flagella (see Table S4).

Expression of stress-related and iron uptake genes was increased in the SCV. The exposure of *P. chlororaphis* SCV to antimicrobials on solid agar, including hydrogen peroxide, revealed a higher level of resistance to oxidative stress than that in the WT strain (Fig. 2B). This indicates that this clonal small-colony variant is especially adapted to oxidative stress. Supporting these results, the key oxidative stress regulator *oxyR* was found to be significantly induced in the SCV (see Table S5 in the supplemental material). This LysR-type redox sensor binds DNA as a dimer while responding to elevated cellular levels of reactive oxygen species (ROS) (26). In *P. aeruginosa*, activated OxyR (encoded by PA5344) stimulates the expression of *katA*, *katB*, *ahpB*, and *ahpCF*, which encode catalases and alkyl-hydroxy peroxidases (27). Besides having a crucial role in upregulating oxidative stress defense, OxyR contributes to *P. aeruginosa* iron acquisition by activating genes involved in pyoverdine biosynthesis and utilization (28). In agreement with these results, five oxidative stress scavenging genes, including *katABG* and *ahpCF*, and 18 iron uptake genes, including *pvd* genes for pyoverdine synthesis and *tonB* and *exb* genes for pyoverdine utilization, were highly expressed in the *P. chlororaphis* SCV (see Table S5).

Validation of RNA-seq. To validate the expression profiles obtained by RNA-seq, quantitative reverse transcription-PCR (qRT-PCR) was performed on 9 selected genes; these included genes encoding components of the quorum-sensing systems; proteins involved in heme, flagellar, phenazine, and pyoverdine synthesis; and enzymes previously shown to detoxify reactive oxygen species. The data (e.g., fold differences in mutant versus WT transcript abundances) from the qRT-PCR analysis were comparable to those obtained by the RNA-seq analysis for all selected genes (see Fig. S1 and Table S2 to S5 in the supplemental material), validating the RNA-seq data.

Genome variation between WT and SCV and complementation analysis. To identify genetic differences between the WT and SCV, the genomes of both strains were sequenced. Notably, a mutation was mapped to a gene annotated as *yfiR* and harboring an in-frame 33-bp deletion in its coding sequence (Table 1). This mutation causes a deletion of 11 amino acids (VLVQRLLADNP) between residues 94 and 104 of YfiR. This periplasmic protein is a negative regulator of cyclic-di-GMP synthesis (13). In *P. aeruginosa*, mutation of *yfiR* results in the accumulation of cyclic-di-GMP and the formation of SCV.

To determine whether the specific genetic mutation in *yfiR* was responsible for the observed phenotypic changes, we expressed

Downloaded from http://aem.asm.org/ on September 11, 2018 by guest

TABLE 1 List of genetic changes in *P. chlororaphis* SCV and phenotypic revertant

Gene identifier	Gene	Protein description	Type	Protein change	Position on protein	Presence in[a]: SCV	Revertant
Pchl3084_0735	*yfiR*	Periplasmic protein	33-bp deletion	In-frame deletion	94–104	+	+
Pchl3084_4816	*cyoE*	Protoheme farnesyltransferase	12-bp insertion	In-frame insertion	208–211	+	+
Pchl3084_0164		Glycosyl hydrolase	SNP	A to T	1188	+	+
				A to T	1190		
				N to D	1197		
				T to A	1208		
				N to D	1214		
Pchl3084_5323	*fusA*	Elongation factor G	SNP	A to V	664	+	+
Pchl3084_1083	*xerD*	Tyrosine recombinase	2-bp insertion	Frame shift	276	−	+
Pchl3084_0637		Precorrin methyltransferase	SNP	R to G	126	−	+
Pchl3084_0840		Hypothetical protein	SNP	N to S	220	−	+
Pchl3084_1162	*cdsA*	Phosphatidate cytidylyltransferase	SNP	F to L	214	−	+
				G to A	219		
Pchl3084_1218		Phage tail protein	SNP	F to Y	320	−	+
				A to D	346		
Pchl3084_3246		Transcriptional regulator	SNP	L to M	318	−	+
				T to P	319		
				V to I	316		
				H to R	208		
Pchl3084_4624	*bifA*	Phosphodiesterase	SNP	V to L	598	−	+

[a] +, presence of mutations; −, absence of mutations.

the wild-type *yfiR* gene in the SCV. The presence of the wild-type *yfiR* gene complemented most SCV phenotypes, including motility, colony size, cell morphology, growth, and biofilm formation (Fig. 3A to E). Phenazine produced by the *yfiR* complemented strain was similar to that produced by the WT (e.g., 3.4 ± 0.3 at OD_{367}). These data indicate that YfiR is responsible for most observed phenotypes in the SCV. Interestingly, the SCV complemented by WT YfiR remained antibiotic resistant, indicating that the antibiotic resistance of the SCV is controlled by other factors.

In addition to the mutation in *yfiR*, other short insertions, deletions, and SNPs were detected (Table 1). In line with the transcriptional analysis, changes were identified in genes annotated as *fusA* (elongation factor G) and *cyoE* (protoheme farnesyltransferase) (Table 1). The *fusA* gene contains an SNP which substitutes an alanine (A) for valine (V) at residue 664. In *Salmonella enterica* serovar Typhimurium, point mutations in the *fusA* gene can lead to an increased resistance to kanamycin and fusidic acid (29). CyoE is involved in the production of heme, a cofactor involved in oxygen-dependent electron chain reaction (30). A previous report showed that the disruption of the electron transport chain reduced the membrane potential and the ability to take up antibiotics, e.g., leading to increased resistance to aminoglycosides (31). An in-frame 12-bp insertion potentially resulted in the addition of 4 amino acids (ILLY) at positions 208 to 211 in CyoE (Table 1). It is possible that changes in the residues in the 6th transmembrane domain by the addition of 4 hydrophobic amino acids alters the conformation of CyoE sufficiently to affect transport (see Fig. S2 and S3 in the supplemental material).

To test the role of FusA in the antibiotic resistance of the SCV, the altered *fusA* from the SCV was introduced into the WT, resulting in increased kanamycin resistance, but not to the level of resistance seen in the SCV (Fig. 3F). However, failure of the altered *fusA* to induce the SCV level of kanamycin resistance when expressed in *trans* in the wild-type background is not unexpected, given the existence of a wild-type copy of *fusA* in the genome. To

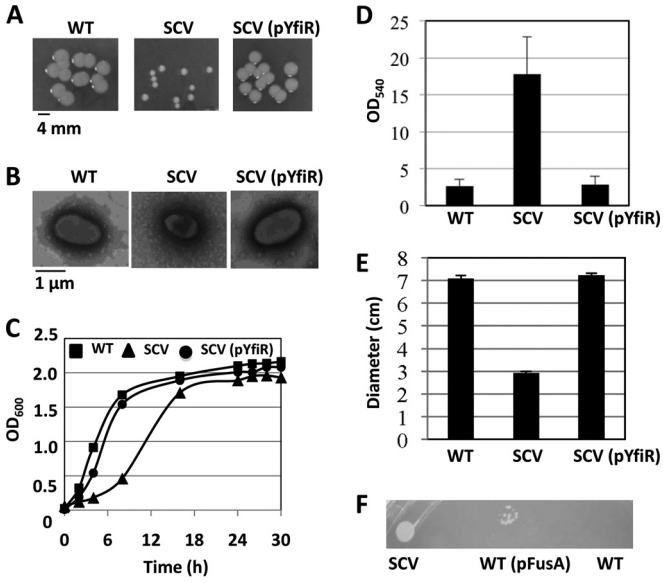

FIG 3 Phenotypes of the *yfiR* and *fusA* complemented strain. (A) Comparison of colony sizes of *P. chlororaphis* WT, SCV, and the *yfiR* complemented strain. Bacteria were grown on LB plates for 3 days. (B) Transmission electron microscopy analysis of cell morphology for *P. chlororaphis* WT, SCV, and the *yfiR* complemented strain. (C) Growth curves of *P. chlororaphis* WT, SCV, and the *yfiR* complemented strain in LB broth at 28°C. Original inocula from stationary cultures were inoculated at a volume-to-volume ratio of 1:1,000. (D) Biofilm formation by *P. chlororaphis* WT, SCV, and the *yfiR* complemented strain. The amount of CV staining was quantified at OD_{540}, and bars indicate SE. Biofilm production was normalized to an OD_{600} of 1 for different strains. (E) Motility comparison of *P. chlororaphis* WT, SCV, and SCV harboring WT *yfiR*. Bacterial strains were spotted at the center of the motility plate (0.25% agar) and incubated at 28°C. Diameters were measured at 32 h postinoculation. (F) Survival rates in response to kanamycin. Similar amounts (OD_{600} = 0.1) of different bacterial strains were inoculated on LB plates containing 10 μg/ml kanamycin. The picture was taken 3 days after inoculation. All data points represent means ± SE from nine biological replicates in three independent experiments.

Downloaded from http://aem.asm.org/ on September 11, 2018 by guest

determine if the mutation of *cyoE* contributed to kanamycin resistance, the WT *cyoE* gene was introduced in *trans* into the SCV. However, the SCV harboring the WT *cyoE* was not decreased in kanamycin resistance (data not shown). These results suggest that *cyoE* mutation does not contribute to the kanamycin resistance in the SCV.

A prominent genetic difference between the WT and the SCV was the deletion in the SCV of an ~70-kb genomic island. This genetic element is the largest one among the three putative mobile genomic islands in *P. chlororaphis* 30-84 (32). The genomic island also is unique to *P. chlororaphis* 30-84 and harbors intact phage integrases (32), which may explain its mobile nature. Interestingly, the genomic island is located at a transition of GC skew and has a low GC content compared to the average value of the whole genome (see Fig. S4 in the supplemental material). This deletion also is supported by the RNA-seq data, since no reads were detected for the 40 genes (Pchl30-84_2928 to Pchl30-84_2967) within this region (see Table S2). Among these genes, 22 are annotated as hypothetical proteins (see Table S6). Twelve genes encode DNA modification/interacting proteins, such as transposases (3 genes), integrases (4 genes), helicase (1 gene), nucleases (2 genes), and transcriptional factors (2 genes). Two genes, *tcdA1* and *tcdC1*, encode functionally uncharacterized insecticidal toxin complex (Tc) proteins. We also designed primers for genes within and flanking this genomic island and confirmed the loss of this genomic island in this SCV (data not shown; also see Table S1).

How or whether this genomic island contributes to the formation of SCV phenotypes remains unclear. Interestingly, loss of the genomic island as determined by PCR was not observed in all SCV isolates obtained from the biofilm (data not shown), suggesting that this loss is not required for the expression of the morphological SCV phenotypes (e.g., small colonies). Furthermore, as discussed above, mutations in *yifR* play a major role in controlling SCV colony size, growth, motility, and biofilm formation in this study. The phenotypes conferred by the loss of this genetic island in the SCV still are not known.

Phenotypic switching and associated genetic alterations. During prolonged incubation of the SCV on swimming motility plates, phenotypic revertants morphologically similar to the WT were isolated from the edge of the swimming circle, and one was further characterized. Analysis revealed that the phenotypic revertant was similar to the WT in colony size, growth rate, biofilm formation, and motility (Fig. 4A to E). However, the phenotypic revertant remained as resistant to kanamycin as the SCV (Fig. 4F). These results suggest that the SCV undergoes partial phenotypic switching, but that the antibiotic resistance phenotype of the SCV can be retained by the revertant. The genome was sequenced to identify the genetic changes that occurred in the phenotypic revertant. As expected, the phenotypic revertant still lacked the 70-kb region, but interestingly it also retained all of the other mutations identified in the SCV (Table 1; also see Fig. S4 in the supplemental material). These results suggest that the phenotypic switching is not due simply to genetic reversion of defects in the SCV genes. Instead, seven other genes containing mutations were identified, demonstrating that compensatory mutation(s) occurring elsewhere in the genome were responsible for phenotypic switching (Table 1). These mutations occurred in *bifA* (phosphodiesterase), *xerD* (tyrosine recombinase), Pchl3084_0637 (precorrin methyltransferase), Pchl3084_0840 (hypothetical protein), *cdsA* (phosphatidate cytidylyltransferase), Pchl3084_1218 (phage tail protein), and Pchl3084_3246 (transcriptional regulator). Because mutations in *bifA* were shown to cause severe defects in swarming motility and a hyperbiofilm phenotype in *P. aeruginosa* (33), we investigated the role of BifA in the SCV phenotypic reversion of *P. chlororaphis*. However, complementation of the SCV with the *bifA* gene from the phenotypic revertant resulted in no measurable changes in phenotypes (data not shown). Future experiments are needed to characterize the contribution of the other genes to the revertant phenotype.

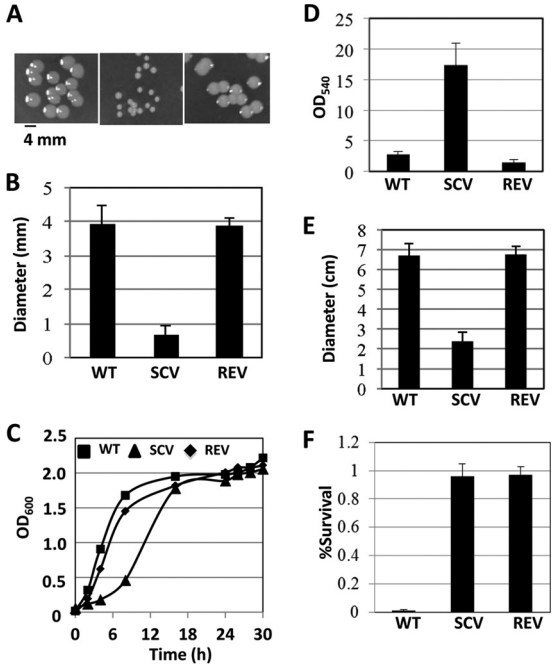

FIG 4 Phenotypes of the phenotypic revertant strain. (A) Comparison of colony sizes of *P. chlororaphis* WT, SCV, and phenotypic revertant strains. Bacteria were grown on an LB plate for 3 days. (B) Colony sizes on LB plates. Different strains were grown at 28°C on an LB agar plate for 3 days. (C) Growth curves of *P. chlororaphis* WT, SCV, and phenotypic revertant strains in LB broth at 28°C. Original inocula from stationary-phase cultures were inoculated at a volume-to-volume ratio of 1:1,000. (D) Biofilm formation by *P. chlororaphis* WT, SCV, and phenotypic revertant strains. Biofilm production was normalized to an OD_{600} of 1 for different strains. (E) Motility comparison of *P. chlororaphis* WT, SCV, and the phenotypic revertant. Bacterial strains were spotted at the center of the motility plate (0.25% agar) and incubated at 28°C. Diameters were measured at 32 h postinoculation. (F) Survival rates in response to kanamycin. All data points represent means ± SE from nine biological replicates in three independent experiments.

DISCUSSION

In this study, an SCV obtained from a biofilm culture has been systematically investigated at the phenotypic, transcriptional, and genomic levels. Changes in growth, motility, and phenazine production, as well as biofilm formation and antimicrobial resistance, correlate well with changes in gene expression as analyzed by genome-wide RNA-seq analysis. In addition, spontaneous mutations in *yfiR* and *fusA* are linked to key phenotypes in the SCV. This confirms that the changes in the SCV across these diverse cellular processes are controlled by genetic variations. Furthermore, phenotypic revertants were recovered that were similar to the WT in colony size, growth rate, biofilm formation, and motility but remained as resistant to kanamycin as the SCV. These

Downloaded from http://aem.asm.org/ on September 11, 2018 by guest

results suggest that the SCV undergoes partial phenotypic switching, but that the antibiotic resistance phenotype of the SCV can be retained by the revertant. This observation has important clinical implications, since phenotypic switching provides a mechanism for the development of antibiotic resistance. These results also highlight the strength of coupled phenotypic and transcriptomic analyses, in combination with whole-genome sequencing, as an approach to unravel complex bacterial adaptations.

A role for cyclic-di-GMP in phenotypic variation has been suggested previously. In *P. aeruginosa* PAO1, an SCV having the characteristic phenotypes (small-colony morphology, decreased motility, and enhanced attachment) emerged as a result of transposon mutagenesis of the cyclic-di-GMP regulator *yfiR*. A model for how YfiR repression of YfiN (TpbB) regulates cyclic-di-GMP levels and SCV formation was proposed (15). Cyclic-di-GMP anabolism is driven by the catalytic activity of GGDEF motif-containing diguanylate cyclases (DGC), such as YifN, which generate c-di-GMP from two molecules of guanosine-5′-triphosphate (GTP). C-di-GMP catabolism is driven by the catalytic activity of EAL motif-containing phosphodiesterases (PDE), which break down c-di-GMP into 5′-phosphoguanylyl-(3′-5′)-guanosine (pGpG) (34). YfiR is a periplasmic protein that serves as a repressor of YfiN (TpbB). Mechanistically it is believed that YfiR binds to YfiN (TpbB) and halts the conversion of the two GTP molecules to c-di-GMP by YfiN (TpbB). Consistent with this model, deletion of *yfiR* in *P. aeruginosa* resulted in increased c-di-GMP levels, linking changes in the c-di-GMP pool to characteristic SCV phenotypes (15). It is hypothesized that c-di-GMP levels control phenotypic changes by interacting with proteins or riboswitches that control gene expression or the activity of enzymes and complex cellular structures (34). It is further speculated that these changes are involved in the transition from motile to nonmotile lifestyles (34). In *P. chlororaphis* 30-84, complementation of the SCV with a wild-type copy of *yfiR* restored the wild-type colony morphology, motility, biofilm formation capability, and growth rate. Although the accumulation of c-di-GMP was not measured, our results are consistent with the *P. aeruginosa* model and suggest that mutation of *yfiR* in the SCV lessened the affinity of *yfiR* to bind to and repress the catalytic activity of YfiN. This would result in the accumulation of c-di-GMP and, ultimately, the SCV phenotype.

Retention of the SCV mutations in *yfiR* in the phenotypic revertant suggested that the revertant phenotype was derived from secondary mutations. We hypothesized that these mutations either affect c-di-GMP levels (e.g., reduce pools to be more similar to wild-type levels) or directly affect phenotypes controlled by c-di-GMP levels, e.g., type IV pili or extracellular polymeric substance production (13, 15, 35). The phenotypic revertant characterized in this study had a point mutation in the gene encoding a well-studied PDE, *bifA* (33, 36). Hypothetically, a mutation that increases the catalytic activity of the PDE *bifA* could counteract the effects of the *yfiR* mutation by breaking down the c-di-GMP that accumulated in the cells as a result of the unregulated catalytic activity of *yfiN* (*tpbB*). Interestingly, the introduction of the revertant copy of *bifA* into the SCV did not result in any noticeable phenotypic changes. These results suggest that the mutation to *bifA* observed in the phenotypic revertant was not responsible for the emergence of the revertant phenotype, and that another mutation(s) observed in the revertant is responsible for the phenotypic change. Future work will include complementation assays to determine the genetic change responsible for the phenotypic reversion.

The SCV characterized in this study was highly resistant to the aminoglycoside kanamycin. The molecular mechanisms of bacterial uptake and resistance to aminoglycosides have been studied extensively. Antibiotic resistance to aminoglycosides typically arises from alterations to the target of aminoglycosidic antibiotic action, the protein synthesis machinery (37, 38). However, the inability of the highly polar aminoglycosidic molecules to cross the outer and inner membranes or the presence of enzymes to inactivate the aminoglycoside also may contribute to resistance (37, 38). To understand the antibiotic resistance phenotype of the SCV and the revertant, we focused on genes that may influence these antibiotic resistance mechanisms. Kanamycin inhibits protein synthesis by binding the 30S ribosome and inhibiting the translocation of the ribosome and proofreading capability of the protein synthesis machinery (37). Previously, mutations to elongation factor G (EF-G) encoded by the gene *fusA* led to slight increases in resistance to kanamycin (29). Elongation factor G is involved in the translocation of the ribosome during protein synthesis, and mutations to EF-G may alter the capability of kanamycin to bind the ribosome to prevent translocation. In *P. chlororaphis* 30-84, the introduction of the altered *fusA* from the SCV in *trans* into the wild type resulted in an increase in resistance to kanamycin. The possibility that changes in antibiotic uptake by the SCV also contributed to antibiotic resistance was suggested by the finding that several genes involved in electron transport were expressed to a much lesser extent in the SCV than in the wild type. The uptake of aminoglycosides into the bacterial cell is dependent on the membrane potential generated by the activity of the electron transport chain (37, 39–42). We hypothesize that the compound effects of decreased expression of electron transport genes will lower the efficiency of the electron transport system, thereby diminishing the membrane potential and the amount of kanamycin taken up by the cell, as has been reported previously (18, 41, 42). The results of this study suggest that antimicrobial resistance in the SCV, the revertant, and the SCV complemented with wild-type *yfiR* is a complex phenotype regulated in part by FusA but likely is the result of a combination of mechanisms.

In the rhizosphere, *P. chlororaphis* must deal with antimicrobials released by plants and microbes, including ROS. Moreover, *P. chlororaphis* must compete with the surrounding microbial communities for nutrients such as iron. The expression of genes involved in ROS detoxification and iron uptake are highly upregulated in the SCV. These data suggest that the SCV are especially adapted to oxidative stress and low iron conditions in the rhizosphere. The increased adherence ability of SCV may enhance its physical association with plant roots or fungal hyphae to better acquire nutrients and live in plant-associated biofilm communities. The prevalence of SCV of *P. chlororaphis* 30-84 and other pseudomonads in both laboratory and natural environments suggests that there is some benefit to the SCV phenotype and some level of selection to maintain this phenotypic variation within the species. Further characterization of genes identified through RNA-seq analysis will provide a more detailed understanding of the genetics of phenotypic switching and the contribution of this mechanism to adaptation of this biological control bacterium.

Downloaded from http://aem.asm.org/ on September 11, 2018 by guest

ACKNOWLEDGMENTS

This project was supported by the Laboratory Directed Research and Development (LDRD) program at Los Alamos National Laboratory and USDA NIFA NRI Competitive Grants project no. 2008-35319-21879.

REFERENCES

1. **Mazzola MR, Cook J, Thomashow LS, Weller DM, Pierson LS, III.** 1992. Contribution of phenazine antibiotic biosynthesis to the ecological competence of fluorescent pseudomonads in soil habitats. Appl Environ Microbiol **58:**2616–2624.
2. **Maddula VSRK, Zhang Z, Pierson EA, Pierson LS, III.** 2006. Quorum sensing and phenazines are involved in biofilm formation by *Pseudomonas chlororaphis* strain 30-84. Microb Ecol **52:**289–301. http://dx.doi.org/10.1007/s00248-006-9064-6.
3. **Dietrich LE, Price-Whelan A, Petersen A, Whiteley M, Newman DK.** 2006. The phenazine pyocyanin is a terminal signaling factor in the quorum sensing network of *Pseudomonas aeruginosa*. Mol Microbiol **61:**1308–1321. http://dx.doi.org/10.1111/j.1365-2958.2006.05306.x.
4. **Audenaert K, Pattery T, Cornelis P, Höfte M.** 2002. Induction of systemic resistance to *Botrytis cinerea* tomato by *Pseudomonas aeruginosa* 7NSK2: role of salicylic acid, pyochelin, and pyocyanin. Mol Plant Microbe Interact **15:**1147–1156. http://dx.doi.org/10.1094/MPMI.2002.15.11.1147.
5. **Rabaey K, Boon N, Siciliano SD, Verhaege M, Verstraete W.** 2005. Microbial phenazine production enhances electron transfer in biofuel cells. Environ Sci Technol **70:**3401–3408. http://dx.doi.org/10.1021/es048563o.
6. **Wang Y, Wilks JC, Danhorn T, Ramos I, Croal L, Newman DK.** 2011. Phenazine-1-carboxylic acid promotes bacterial biofilm development via ferrous iron acquisition. J Bacteriol **193:**3606–3617. http://dx.doi.org/10.1128/JB.00396-11.
7. **Folsom JP, Richards L, Pitts B, Roe F, Ehrlich GD, Parker A, Mazurie A, Stewart PS.** 2010. Physiology of *Pseudomonas aeruginosa* in biofilms as revealed by transcriptome analysis. BMC Microbiol **10:**294. http://dx.doi.org/10.1186/1471-2180-10-294.
8. **Hentzer M, Eberl L, Givskov M.** 2005. Transcriptome analysis of *Pseudomonas aeruginosa* biofilm development: anaerobic respiration and iron limitation. Biofilms **2:**37–61. http://dx.doi.org/10.1017/S1479050505001699.
9. **Deziel E, Comeau Y, Villemur R.** 2001. Initiation of biofilm formation by *Pseudomonas aeruginosa* 57RP correlates with emergence of hyperpiliated and highly adherent phenotypic variants deficient in swimming, swarming, and twitching motilities. J Bacteriol **183:**1195–1204. http://dx.doi.org/10.1128/JB.183.4.1195-1204.2001.
10. **Chancey S, Wood D, Pierson EA, Pierson LS, III.** 2002. Survival of GacS/GacA mutants of the biological control bacterium *Pseudomonas aureofaciens* 30-84 in the wheat rhizosphere. Appl Environ Microbiol **68:**3308–3314. http://dx.doi.org/10.1128/AEM.68.7.3308-3314.2002.
11. **Wei Q, Tarighi S, Dötsch A, Haussler S, Müsken M, Wright VJ, Camara M, Williams P, Haenen S, Boerjan B, Bogaerts A, Vierstraete E, Verleyen P, Schoofs L, Willaert R, Groote VN, Michiels J, Vercammen K, Crabbe A, Cornelis P.** 2011. Phenotypic and genome-wide analysis of an antibiotic-resistant small colony variant (SCV) of *Pseudomonas aeruginosa*. PLoS One **6:**e29276. http://dx.doi.org/10.1371/journal.pone.0029276.
12. **Haussler S, Ziegler A, Lottel F, von Gotz M, Rohde D, Wehmhohner S, Saravanamuthu B, Tummler B, Steinmetz I.** 2003. Highly adherent small-colony variants of *Pseudomonas aeruginosa* in cystic fibrosis lung infection. J Med Microbiol **52:**295–301. http://dx.doi.org/10.1099/jmm.0.05069-0.
13. **Malone JG, Jaeger T, Manfredi P, Dotsch A, Blanka A, Bos R, Cornelis GR, Haussler S, Jenal U.** 2012. The YfiBNR signal transduction mechanism reveals novel targets for the evolution of persistent *Pseudomonas aeruginosa* in cystic fibrosis airways. PLoS Pathog **8:**e1002760. http://dx.doi.org/10.1371/journal.ppat.1002760.
14. **Workentine ML, Harrison JJ, Weljie AM, Tran VA, Stenroos PU, Tremaroli V, Vogel HJ, Ceri H, Turner RJ.** 2010. Phenotypic and metabolic profiling of colony morphology variants evolved from *Pseudomonas fluorescens* biofilms. Environ Microbiol **12:**1565–1577. http://dx.doi.org/10.1111/j.1462-2920.2010.02185.x.
15. **Malone JG, Jaeger T, Spangler C, Ritz D, Spang A, Arrieumerlou C, Kaever V, Landmann R, Jenal U.** 2010. YfiBNR mediates cyclic di-GMP dependent small colony variant formation and persistence in *Pseudomonas aeruginosa*. PLoS Pathog **6**(3)**:**e1000804. http://dx.doi.org/10.1371/journal.ppat.1000804.
16. **Pu M, Wood TK.** 2010. Tyrosine phosphatase TpbA controls rugose colony formation in *Pseudomonas aeruginosa* by dephosphorylating diguanylate cyclase TpbB. Biochem Biophys Res Commun **402**(2)**:**351–355. http://dx.doi.org/10.1016/j.bbrc.2010.10.032.
17. **von Götz F, Häussler S, Jordan D, Saravanamuthu SS, Wehmhöner D, Strüssmann A, Lauber J, Attree I, Buer J, Tummler B, Steinmetz I.** 2004. Expression analysis of a highly adherent and cytotoxic small colony variant of *Pseudomonas aeruginosa* isolated from a lung of a patient with cystic fibrosis. J Bacteriol **186:**3837–3847. http://dx.doi.org/10.1128/JB.186.12.3837-3847.2004.
18. **Proctor RA, von Eiff C, Kahl BC, Becker K, McNamara P, Herrmann M, Peters G.** 2006. Small colony variants: a pathogenic form of bacteria that facilitates persistent and recurrent infections. Nat Rev Microbiol **4:**295–305. http://dx.doi.org/10.1038/nrmicro1384.
19. **Wang D, Yu J, Pierson LS, Pierson EA.** 2012. Differential regulation of phenazine biosynthesis by RpeA and RpeB in *Pseudomonas chlororaphis* strain 30-84. Microbiology **158:**1745–1757. http://dx.doi.org/10.1099/mic.0.059352-0.
20. **Pierson LS, III, Thomashow LS.** 1992. Cloning and heterologous expression of the phenazine biosynthetic locus from *Pseudomonas aureofaciens* 30-84. Mol Plant Microbe Interact **5:**330–339. http://dx.doi.org/10.1094/MPMI-5-330.
21. **Wang D, Lee SH, Seeve C, Yu J, Pierson LS, III, Pierson EA.** 2013. Roles of the Gac-Rsm pathway in the regulation of phenazine biosynthesis in *Pseudomonas chlororaphis* 30-84. Microbiologyopen **2:**505–524. http://dx.doi.org/10.1002/mbo3.90.
22. **Robinson MD, McCarthy DJ, Smyth GK.** 2010. edgeR: a Bioconductor package for differential expression analysis of digital gene expression data. Bioinformatics 26:139–140. http://dx.doi.org/10.1093/bioinformatics/btp616.
23. **Wang D, Han CS, Dichosa AEK, Gleasner CD, Johnson SL, Daligault HE, Davenport KW, Li P-E, Pierson EA, Pierson LS, III.** 2013. Draft genome sequence of *Pseudomonas putida* strain S610, a seed-borne bacterium of wheat. Genome Announc **1**(6)**:**e01048-13. http://dx.doi.org/10.1128/genomeA.01048-13.
24. **Li H, Durbin R.** 2009. Fast and accurate short read alignment with Burrows-Wheeler transformation. Bioinformatics **25:**1754–1760. http://dx.doi.org/10.1093/bioinformatics/btp324.
25. **Omsland AD, Cockrell C, Fischer ER, Heinzen RA.** 2008. Sustained axenic metabolic activity by the obligate intracellular bacterium *Coxiella burnetii*. J Bacteriol **190:**3203–3212. http://dx.doi.org/10.1128/JB.01911-07.
26. **Choi HJ, Kim SJ, Mukhopadhyay P, Cho S, Woo JR, Storz G, Ryu SE.** 2001. Structural basis of the redox switch in the OxyR transcription factor. Cell **105:**103–113. http://dx.doi.org/10.1016/S0092-8674(01)00300-2.
27. **Ochsner UA, Vasil ML, Alsabbagh E, Parvatiyar K, Hassett DJ.** 2000. Role of the *Pseudomonas aeruginosa oxyR-recG* operon in oxidative stress defense and DNA repair: OxyR-dependent regulation of *katB-ankB*, *ahpB*, and *ahpC-ahpF*. J Bacteriol **182:**4533–4544. http://dx.doi.org/10.1128/JB.182.16.4533-4544.2000.
28. **Vinckx T, Matthijs S, Cornelis P.** 2008. Loss of the oxidative stress regulator OxyR in *Pseudomonas aeruginosa* PAO1 impairs growth under iron-limited conditions. FEMS Microbiol Lett **288:**258–265. http://dx.doi.org/10.1111/j.1574-6968.2008.01360.x.
29. **Johanson U, Hughes D.** 1994. Fusidic acid-resistant mutants define three regions in elongation factor G of *Salmonella typhimurium*. Gene **143:**55–59. http://dx.doi.org/10.1016/0378-1119(94)90604-1.
30. **Saiki K, Mogi T, Anraku Y.** 1992. Heme O biosynthesis in *Escherichia coli*: the *cyoE* gene in the cytochrome *bo* operon encodes a protoheme IX farnesyltransferase. Biochem Biophys Res Commun **189:**1491–1497. http://dx.doi.org/10.1016/0006-291X(92)90243-E.
31. **Bryan LE, Kwan S.** 1983. Roles of ribosomal binding, membrane potential, and electron transport in bacterial uptake of streptomycin and gentamycin. Antimicrob Agents Chemother **23:**835–845. http://dx.doi.org/10.1128/AAC.23.6.835.
32. **Loper JE, Hassan KA, Mavrodi D, Davis EW, II, Lim CH, Shaffer BT, Elborne LDH, Stockwell VO, Hartney SL, Breakwell K, Henkels MD, Tetu SG, Rangel LI, Kidarsa TA, Wilson NL, van Mortel J, Song C, Blumhagen R, Radune D, Hostetler JB, Brinkac LM, Durkin AS, Kluepfel DA, Wechter WP, Anderson AJ, Kim YC, Pierson LS, III, Pierson**

Downloaded from http://aem.asm.org/ on September 11, 2018 by guest

EA, Lindow SE, Raaijmakers JM, Weller DM, Thomashow LS, Allen AE, Paulsen IT. 2012. Comparative genomics of plant-associated *Pseudomonas* spp.: insights into diversity and inheritance of traits involved in multitrophic interactions. PLoS Genet **8:**e1002784. http://dx.doi.org/10.1371/journal.pgen.1002784.

33. **Kuchma SL, Brothers KM, Merritt JH, Liberati NT, Ausubel FM, O'Toole GA.** 2007. BifA, a cyclic-di-GMP phosphodiesterase, inversely regulates biofilm formation and swarming motility by *Pseudomonas aeruginosa* PA14. J Bacteriol **189:**8165–8178. http://dx.doi.org/10.1128/JB.00586-07.
34. **Hengge R.** 2009. Principles of c-di-GMP signaling in bacteria. Nat Rev Microbiol **7:**263–273. http://dx.doi.org/10.1038/nrmicro2109.
35. **Ha DG, Richman ME, O'Toole GA.** 2014. Deletion mutant library for investigation of functional outputs of cyclic digunylate metabolism in *Psuedomonas aeruginosa* PA14. Appl Environ Microbiol **80:**3384–3393. http://dx.doi.org/10.1128/AEM.00299-14.
36. **Jimenez-Fernandez A, Lopez-Sanchez A, Calero P, Govantes F.** 2014. The c-di-GMP phosphodiesterase BifA regulates biofilm development in *Pseudomonas putida*. Environ Microbiol Rep **1:**208–211. http://dx.doi.org/10.1111/1758-2229.12153.
37. **Mingeot-Leclerco MP, Glupczynski Y, Tulkens PM.** 1999. Aminoglycosides: activity and resistance. Antimicrob Agents Chemother **43:**727–737.
38. **Whiteley M, Bangera MG, Bumgarner RE, Parsek MR, Teltzel GM, Lory S, Greenberg EP.** 2001. Gene expression in *Pseudomonas aeruginosa* biofilms. Nature **413:**860–864. http://dx.doi.org/10.1038/35101627.
39. **Rutherford K, Parkhill J, Crook J, Horsnell T, Rice P, Rajandream MA, Barrell B.** 2000. Artemis: sequence visualization and annotation. Bioinformatics **10:**944–945. http://dx.doi.org/10.1093/bioinformatics/16.10.944.
40. **Stewart PS, Costerton JW.** 2001. Antibiotic resistance of bacteria in biofilms. Lancet **358:**135–138. http://dx.doi.org/10.1016/S0140-6736(01)05321-1.
41. **Taber HW, Mueller JP, Miller PF, Arrow AS.** 1987. Bacterial uptake of aminoglycoside antibiotics. Microbiol Rev **51:**439–457.
42. **Proctor RA, Humboldt AV.** 1998. Bacterial energetics and antimicrobial resistance. Drug Resist Updat **1:**227–235. http://dx.doi.org/10.1016/S1368-7646(98)80003-4.

Downloaded from http://aem.asm.org/ on September 11, 2018 by guest